Springer

Journal of
Mechanical
Science and
Technology

Journal of Mechanical Science and Technology 22 (2008) 460~468

www.springerlink.com/content/1738-494x

Vibration characteristics of computer stacked disks and head assembly

Shyh-Chin Huang* and Kao-An Lin

Department of Mechanical Engineering, National Taiwan University of Science and Technology, 43, Keelung Road, Sec.4, Taipei, Taiwan 106.

(Manuscript Received March 16, 2007; Revised November 6, 2007; Accepted November 10, 2007)

Abstract

A stacked multi-disk with read/write head assembly was investigated. The interference of head assembly on the spinning disks was modeled by stationary springs intervening between disks. The receptance method was then applied to join the spinning disks and the stationary springs. A general, recursive equation for natural frequency of a disk-head system was derived. Numerical examples followed for the cases of 3 to 6 stacked disks. The results showed that even for weak spring coupling, the changes of mode shapes were very significant and the changes of natural frequencies were slight. The effects of spring stiffness, location, and disk spinning speed were examined as well. The spinning speed was seen to pull the frequency loci to pass through the crossings of a single disk's frequency curves and there existed a curve-veering phenomenon.

Keywords: Spinning stacked disks; Computer drive; Coupling vibrations; Receptance method

1. Introduction

Spinning disks have been widespread in engineering applications, e.g., saw blades, turbine rotors, and computer disks. Some typical publications are described in the following. Lamb and Southwell [1] derived the equations for a spinning disk and solved for its natural frequencies and mode shapes. Mote [2] used the Rayleigh-Ritz method to solve for the case of a disk with initial stresses. Adams [3] discussed the critical speeds of a spinning disk.

Since the early1970's, due to the rise of computer technology, researches on spinning disks have been mainly focused on simulating hard disk drives. The most crucial part encountered in the disk-head assembly is the interaction between spinning disk and read/write head. Benson and Bogy [4] treated the head as a stationary transverse load. Stahl and Iwan [5,6] modeled the disk as a rigid element but of two/three degree-of-freedom and the head was modeled as a counter-spinning mass. Shen and Mote [7] modeled the head as a spring-mass-dashpot (SMD) counter rotating on a stationary disk. Chen and Bogy examined the natural frequencies and stability of a spinning disk with a stationary load system [8], and then extended it to allow a disk's rigid body tilting [9]. Huang and Chiou [10] first considered the moving effect of the head and modeled it as a radially moving load.

In accordance with the development of stacked hard disks, the investigations of spinning multi-disk have gained more attention since the1990's. Shen and Ku [11] and Shen [12] investigated the vibration characteristics of spinning multi-disk/spindle systems, in which the spindle was allowed to have rigid tilting. They concluded that the rigid tilting was coupled to the disk's one nodal diameter mode. The interaction of head and disks was not yet addressed. Orgun and Tongue [13] examined a multi-disk computer drive, in which circular plates were coupled together through discrete springs. In that paper the disks and springs rotated together; however, that was unlike a real disk drive where the head did not spin. In a later

*Corresponding author. Tel.: +82 2 2737 6443, Fax.: +82 2 2737 6460
E-mail address: schuang@mail.ntust.edu.tw
DOI 10.1007/s12206-007-1104-8

paper [14], they improved the model to have stationary springs on spinning disks. In the above two papers, the Rayleigh-Ritz method was employed and the mode localization due to individual disk thickness disorder was emphasized. The authors of those papers discussed the cases of weak to strong coupling and concluded that the occurrence of mode localization depended on the disorder to coupling ratio, rather than the degree of disorder. They also found the spring might cause instability under the condition that a backward traveling wave coincided with a reflected wave.

The present research is devoted to developing a systematic approach for the vibration of a stacked disks-head assembly, and to examine its natural frequencies, mode shapes, and coupling effects. The difficulty that arises from this system is the connection between stationary and spinning elements. The first author of the present paper has derived the receptance theory to join rotating and stationary elements (Huang and his co-researchers [15-17]). That method is to be applied and eventually a very neat and general formula for natural frequencies and mode shapes is derived. The coupling effects due to spring constant, spring location, and spinning speed are then discussed.

2. Frequency equation and mode shapes

Fig. 1(a) shows a schematic diagram of a stacked multi-disk unit in a computer storage system. The read/write heads are suspended to the tips of cantilevered arms that are fixed to a relatively stiff foundation. A simplified model is shown in Fig. 1(b), in which springs intervene between disks. Since the head assembly is of stiff foundation, the coupling among disks, to the authors' opinion, is relatively weak, the same remarks as made by Orgun and Tonque [13, 14]. The present system is similar to the study conducted by Orgun and Tonque [13] but by a thoroughly different approach. In addition, unlike that of Orgun and Tonque [13], the present study focuses on the vibration characteristics due to coupling rather than the localization due to thickness disorder.

Fig. 2 shows a spinning disk, in which (X,Y,Z) is an inertia frame; a, the outer radius; b the inner radius; Ω, the spinning speed; ϕ, the angular coordinate with respect to the inertia frame. The equation of motion of a spinning disk in terms of its transverse displacement u (r,ϕ,t) with respect to a stationary observer was derived [15]

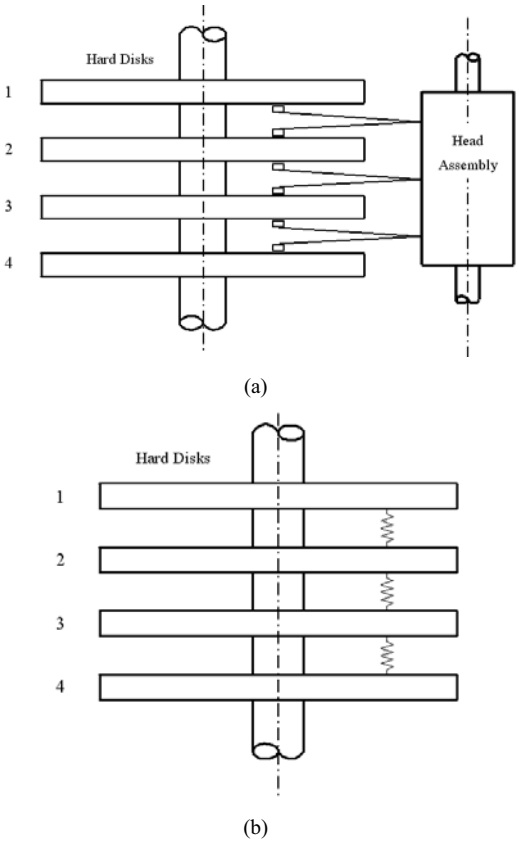

Fig. 1. (a) Schematic diagram of stacked hard disks and head assembly, and (b) a simplified model.

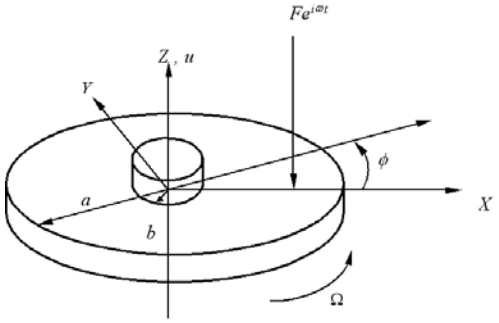

Fig. 2. Schematic diagram and coordinates of a spinning disk.

$$D\left(\frac{\partial^2}{\partial r^2}+\frac{\partial}{r\partial r}+\frac{1}{r^2}\frac{\partial^2}{\partial\phi^2}\right)^2 u$$
$$-\frac{h}{r}\left[\frac{\partial}{\partial r}\left(r\sigma_r\frac{\partial u}{\partial r}\right)+\frac{\partial}{r\partial\phi}\left(\sigma_\phi\frac{\partial u}{\partial\phi}\right)\right]$$
$$+\rho h\left[\frac{\partial^2 u}{\partial t^2}+2\Omega\frac{\partial^2 u}{\partial\phi\partial t}+\Omega^2\frac{\partial^2 u}{\partial\phi^2}\right]=p(r,\phi,t), \quad (1)$$

where $D=Eh^3/12\,(1-\nu^2)$, the bending rigidity; ρ, den-

sity; h, thickness; ν, Poisson's ratio; p pressure type loading; σ^r and σ^ϕ, initial stresses due to spin,

$$\sigma_r(r)=\frac{(3+\nu)}{8}\rho\Omega^2(a^2-r^2)+\frac{\rho\Omega^2b^2(1-\nu)[a^2(3+\nu)-b^2(1+\nu)]}{8[b^2(1-\nu)+a^2(1+\nu)]}(\frac{a^2}{r^2}-1) \quad (2)$$

$$\sigma_\phi(r)=\frac{\rho\Omega^2}{8}[(3+\nu)a^2-(1+3\nu)r^2]-\frac{\rho\Omega^2b^2(1-\nu)[a^2(3+\nu)-b^2(1+\nu)]}{8[b^2(1-\nu)+a^2(1+\nu)]}(\frac{a^2}{r^2}+1) \quad (3)$$

The disk is assumed clamped inside and free outside, *i.e.,*

$$\begin{cases} M_{rr}(a,\phi,t)=0 \\ V_{rr}(a,\phi,t)=0 \\ u(b,\phi,t)=0 \\ \dfrac{\partial u(b,\phi,t)}{\partial r}=0 \end{cases} \quad (4)$$

where the bending moments and effective shear forces are

$$M_{rr}=-D[\frac{\partial^2u}{\partial r^2}+\nu(\frac{1}{r}\frac{\partial u}{\partial r}+\frac{1}{r^2}\frac{\partial^2u}{\partial\phi^2})] \quad (5)$$

$$V_{rr}=Q_r+\frac{1}{r}\frac{\partial M_{r\phi}}{\partial\phi} \quad (6)$$

$$Q_r=-D\frac{\partial}{\partial r}(\nabla^2u) \quad (7)$$

$$M_{r\theta}=-D(1-\nu)\frac{\partial}{\partial r}(\frac{1}{r}\frac{\partial u}{\partial\phi}) \quad (8)$$

By the traveling modes expansion [15], a disk's displacement function can be assumed to be

$$u(r,\phi,t)=\sum_{m=0}^{M}\sum_{n=0}^{N}\eta_{mn}(t)\cdot R_{mn}(r)e^{i(n\phi+\omega_{mn}t)}=\sum_{m=0}^{M}\sum_{n=0}^{N}[q^c_{mn}(t)\cos n\phi+q^s_{mn}(t)\sin n\phi]R_{mn}(r)\,, \quad (9)$$

where m, nodal circle number; n, nodal diameter number; M, N, the terms deemed necessary for numerical accuracy; $R_{mn}(r)$ is the radial function and is here chosen the beam function, *i.e.*,

$$R_{mn}(r)=[\sin\beta_{mn}(r-b)-\sinh\beta_{mn}(r-b)]+\alpha_{mn}[\cos\beta_{mn}(r-b)-\cosh\beta_{mn}(r-b)] \quad (10)$$

Note that Eq. (10) by itself satisfies the inner clamped boundary and α_{mn}, β_{mn} are two parameters chosen to satisfy the outer boundary.

Substitute Eq. (9) into Eq. (1), employ the Galerkin's method, and utilize the orthogonality of trigonometric functions, the modal participation factors for each n number can be decoupled and solved for from the following equations:

$$[\mathrm{T}_{sm0}]\{\ddot{q}^c_{m0}\}+[\Phi_{sm0}]\{q^c_{m0}\}=\{Q^c_{s0}\} \quad \text{for } n=0 \quad (11)$$

and for $n\neq0$,

$$[\mathrm{T}_{smn}]\{\ddot{q}^c_{mn}\}+2n\Omega[\mathrm{T}_{smn}]\{\dot{q}^s_{mn}\}+([\Phi_{smn}]-n^2\Omega^2[\mathrm{T}_{smn}])\{q^c_{mn}\}=\{Q^c_{sn}\} \quad (12)$$

$$[\mathrm{T}_{smn}]\{\ddot{q}^s_{mn}\}-2n\Omega[\mathrm{T}_{smn}]\{\dot{q}^c_{mn}\}+([\Phi_{smn}]-n^2\Omega^2[\mathrm{T}_{smn}])\{q^s_{mn}\}=\{Q^s_{sn}\} \quad (13)$$

where s,m=0,1,….,M. The above matrices are of dimension (M+1)× (M+1) and their entries are

$$\mathrm{T}_{smn}=\int_b^a R_{mn}(r)R_{sn}(r)r\,dr \quad (14)$$

$$\Phi_{smn}=\frac{1}{\rho h}\left\{D\int_b^a\{[(\frac{d^2}{dr^2}+\frac{d}{rdr}-\frac{n^2}{r^2})^2R_{mn}(r)]\cdot R_{sn}(r)\}r\,dr-h\int_b^a\{[\frac{d}{dr}(r\sigma_r\frac{dR_{mn}(r)}{dr})-\frac{n^2}{r}\sigma_\phi R_{mn}(r)]\cdot R_{sn}(r)\}dr\right\} \quad (15)$$

$$Q^c_{s0}=\frac{1}{2\rho h\pi}\int_b^a\int_0^{2\pi}R_{s0}(r)p(r,\phi,t)r\,d\phi\,dr \quad (16)$$

$$Q^c_{sn}=\frac{1}{\rho h\pi}\int_b^a\int_0^{2\pi}R_{sn}(r)p(r,\phi,t)\cos(n\phi)r\,d\phi\,dr \quad (17)$$

$$Q^s_{sn}=\frac{1}{\rho h\pi}\int_b^a\int_0^{2\pi}R_{sn}(r)p(r,\phi,t)\sin(n\phi)r\,d\phi\,dr \quad (18)$$

Equations (11-13) enable us to solve for the modal participation factors, separately, for each n number. The selection of M relies on the frequency range of interest. For cases where only the lower frequency range is of interest one may just take the zero (s=m=0) nodal circle modes such that Eqs. (11-13) are further simplified to

$$\ddot{q}^c_0(t)+\Psi^2_0q^c_0(t)=\frac{Q^c_0}{\mathrm{T}_0},\quad n=0 \quad (19)$$

$$\begin{Bmatrix}\ddot{q}^c_n\\ \ddot{q}^s_n\end{Bmatrix}+\begin{bmatrix}0 & 2n\Omega\\ -2n\Omega & 0\end{bmatrix}\begin{Bmatrix}\dot{q}^c_n\\ \dot{q}^s_n\end{Bmatrix}+\begin{bmatrix}\Psi^2_n-n^2\Omega^2 & 0\\ 0 & \Psi^2_n-n^2\Omega^2\end{bmatrix}\begin{Bmatrix}q^c_n\\ q^s_n\end{Bmatrix}=\frac{1}{\mathrm{T}_n}\begin{Bmatrix}Q^c_n\\ Q^s_n\end{Bmatrix},n\neq0 \quad (20)$$

where $\Psi^2_n=\Phi_n/\mathrm{T}_n$.

Solving the above equations for the disk's natural frequencies, one obtains

$$\omega_{n1} = n\Omega - \Psi_n \tag{21}$$

$$\omega_{n2} = n\Omega + \Psi_n \tag{22}$$

where $\omega_{n1,2}$ are the natural frequencies of the (m,n)=$(0,n)$ modes, one forward (+) and one backward (-), as viewed by a stationary observer. It can be proven that Ψ_n is the disk's natural frequency as viewed from the rotating coordinates.

The receptance method is applied to connect the stacked disks and springs. This method requires the calculation of harmonic force responses of all elements. It is hence assumed a harmonic point force of magnitude F applied at the disk's location (r_0, ϕ_0),

$$p(r,\phi,t) = \frac{F}{r}\delta(r-r_0)\delta(\phi-\phi_0)e^{i\omega t} \tag{23}$$

Subsequently, the disk's response is solved for from previous development,

$$\begin{aligned} u(r,\phi,t) = \sum_{n=0}^{N} & \frac{Fe^{i\omega t}R_n(r_0)R_n(r)}{\mu\rho h \mathrm{T}_n(\omega^2-\omega_{n1}^2)(\omega_{n2}^2-\omega^2)} \\ & \{(\omega_{n1}\omega_{n2}+\omega^2)\cos n(\phi-\phi_0) \\ & -i[\omega(\omega_{n2}+\omega_{n1})\sin n(\phi-\phi_0)]\} \end{aligned}$$

$$\mu = \begin{cases} 2\pi & n=0 \\ \pi & n\neq 0 \end{cases} \tag{24}$$

The receptance α_{ij} is defined as the ratio of displacement output at (r_i, ϕ_i) to a harmonic point force input at (r_j, ϕ_j) and from Eq. (24) it is calculated to be

$$\alpha_{ij} = \Re_{ij} + i\Im_{ij} \ , \tag{25}$$

with

$$\Re_{ij}(\omega) = \sum_{n=0}^{N} \frac{R_n(r_i)R_n(r_j)\left\{(\omega_{n1}\omega_{n2}+\omega^2)\cos[n(\phi_i-\phi_j)]\right\}}{\mu\rho h \mathrm{T}_n(\omega^2-\omega_{n1}^2)(\omega_{n2}^2-\omega^2)}, \tag{26}$$

$$\Im_{ij}(\omega) = \sum_{n=0}^{N} \frac{-R_n(r_i)R_n(r_j)\left\{\omega(\omega_{n2}+\omega_{n1})\sin[n(\phi_i-\phi_j)]\right\}}{\mu\rho h \mathrm{T}_n(\omega^2-\omega_{n1}^2)(\omega_{n2}^2-\omega^2)}. \tag{27}$$

Note that the cross receptances for a spinning structure had been proven [15] to be in complex conjugate pairs. The direct receptance yet is always a real number, *i.e.*,

$$\alpha_{ii}(\omega) = \sum_{n=0}^{N} \frac{R_n^2(r_i)(\omega_{n1}\omega_{n2}+\omega^2)}{\mu\rho h \mathrm{T}_n(\omega^2-\omega_{n1}^2)(\omega_{n2}^2-\omega^2)} \tag{28}$$

In a similar manner, the receptance of a discrete spring is

$$\beta_{ii} = \frac{1}{k_i} \tag{29}$$

Since in the present system, only the direct receptances are to be used, one subscript rather than two is used hereafter for simplicity. Considering a general p-disk with p-1 springs in between, the authors apply the equilibrium and compatibility relations and derive the frequency equation to be

$$(1/\alpha_p)+\cfrac{1}{(1/k_{p-1})+\cfrac{1}{(1/\alpha_{p-1})+\cfrac{1}{(1/k_{p-2})+\cfrac{1}{(1/\alpha_{p-2})+\cfrac{1}{\ddots \cfrac{1}{(1/k_1)+\cfrac{1}{(1/\alpha_1)}}}}}}} = 0 \tag{30}$$

where α_j denotes the j$^{\text{th}}$ disk's receptance and k_j denotes the j^{th} spring constant. Eq. (30) enables us to solve for the natural frequencies, said ω_k's, of the coupled system. To sketch the associated mode shape the modal forces connecting disks and springs must be calculated from the following equation:

$$\begin{bmatrix} \alpha_1+\gamma_1 & \alpha_2 & 0 & 0 & \cdots & \cdots & 0 \\ \alpha_2 & \alpha_2+\gamma_2 & \alpha_3 & 0 & \cdots & \cdots & 0 \\ 0 & \alpha_3 & \alpha_3+\gamma_3 & \alpha_4 & \cdots & \cdots & 0 \\ \vdots & \vdots & \vdots & \ddots & & & \vdots \\ \vdots & \vdots & \vdots & & \ddots & & 0 \\ \vdots & \vdots & \vdots & & & \ddots & \alpha_{p-1} \\ 0 & \cdots & \cdots & \cdots & 0 & \alpha_{p-1} & \gamma_{p-1}+\alpha_p \end{bmatrix}_{\omega=\omega_k} \begin{Bmatrix} F_1 \\ F_2 \\ F_3 \\ \vdots \\ \vdots \\ \vdots \\ F_{p-1} \end{Bmatrix} = 0 \tag{31}$$

where $\gamma_i = \alpha_{i+1} + \dfrac{1}{k_i}$ (32)

Eq. (32) is solved for the force ratios among springs, and these forces are applied as external excitations to the disks. The disks' responses exactly reflect the corresponding mode shapes.

3. Numerical results

In the following, the cases of up to six stacked disks are illustrated. The disks and springs are assumed identical. That is yet an unnecessary restraint since the approach is very general in every aspect. If the effects of disorder in a disk as discussed by Orgun

and Tonque [13, 14] or a mistuned spring are of interest, one may just substitute the parameters into the corresponding receptances in Eqs. (30, 31) to examine its localization phenomena. The geometrical and material properties and the obtained first four natural frequencies (m=0, n=1,0,2,3) of a single disk are listed in Table 1. In order to present the data with less dimensional dependence, the following dimensionless parameters are defined: $\omega^* = \omega/(\rho h a^4/D)$, $\Omega^* = \Omega/(\rho h a^4/D)$, $k^* = k/[D/(a-b)^2]$, respectively, represent the normalized natural frequency, spinning speed, and spring constant. In Table 1, the obtained disk's natural frequencies are compared to those of Vogel [18] and of Lessia [19], and satisfactory agreement was seen.

The coupling among disks is relatively weak if computer hard disks are addressed. Very weak coupling is expected to slightly alter the natural frequencies. To magnify the coupling influence on mode shapes, the authors select a mild spring constant of k^*=10 in the following examples and the effects of spring constant on natural frequencies changes are then illustrated in separate plots. Table 2 shows the first three mode sets for the cases of three to six stacked disks. The modes evolved from the same disk mode, *e.g.*, n=1, are grouped into a set and assigned one set number, *e.g.*, 1. In each set an alphabetic letter follows the number, *e.g.*, 1a, 1b, in an ascending order of frequencies, to distinguish individual modes. From Table 2 it is first seen that for p-stacked disks there exist p natural frequencies in each set and the first natural frequency of a set is exactly equal to that of a single disk. That means that under that frequency, the springs impose no effect at all. It will be shown from the mode shape that the result is correct since all disks deform the same and vibrate in phase so that the springs undergo no deformation. The reason that there exist p natural frequencies for p-stacked disks is explained as follows. When the p disks were not connected through springs, the system existed with p clustering (repeated) natural frequencies for each (m,n) mode. The intervening of springs interconnects the disks so that the originally repeated natural frequency evolves into p distinct natural frequencies. Fig. 3 illustrates the mode shapes of the first set for the 3-disk case. The rectangular plots on the left show the transverse deformation of disks at the cross-sections of spring connections, and the disk deformation is shown on the right by contour plots. These three modes correspond to (m,n)= (0,1). At (1a) mode, three disks undergo the same vibration such that the springs experience no deformation and the original disk's natural frequency retains. At (1b) mode, the top and bottom disks undergo the same vibration but anti-phase. The middle disk is in balance and has no deformation. In contrast to (1b), at (1c) mode three disks vibrate in phase but the middle one has double magnitude such that the two springs are one elongated, one compressed in every moment. Similar modes are observed for the second (n=0) and the third set (n=2). Modes (1b,1c) have revealed the interesting phenomenon that although these two modes belong to n=1 it no longer remains a nodal diameter. The spring coupling alters it to become two nodal radii symmetric to spring location, even though the natural frequency varies just slightly.

Fig. 4 shows the first set of the 4-disk case. As depicted previously, at the first mode, all disks vibrate in phase. At the second mode, the top and bottom disks

Table 1. Disk properties and first four natural frequencies.

Density	$\rho = 1.3\times10^3\, kg/m^3$
Modulus	$E = 4.9\times10^9\, N/m^2$
Poisson ratio	$\nu = 0.3$
Thickness	$h = 0.078mm$
Outer radius	$a = 65.0mm$
Inner radius	$b = 19.5mm$
Natural frequencies ω^*(m=0,n=1,0,2,3)	6.557, 6.663, 7.968, 13.288

Table 2. ω^* for 3 to 6 stacked disks ($\Omega^* = 0$, $k^* = 10$, $r_0 = (a-b)/2$).

	Natural frequencies (ω^*)					
Disk No.	First set		Second set		Third set	
3	1a	6.5574	2a	6.6629	3a	7.9684
	1b	6.6215	2b	7.0059	3b	8.3550
	1c	6.6246	2c	7.2607	3c	9.2636
4	1a	6.5574	2a	6.6629	3a	7.9684
	1b	6.6180	2b	6.8792	3b	8.1769
	1c	6.6239	2c	7.1796	3c	8.8221
	1d	6.6248	2d	7.2819	3d	9.4293
5	1a	6.5574	2a	6.6629	3a	7.9684
	1b	6.6135	2b	6.8011	3b	8.0976
	1c	6.6228	2c	7.0896	3c	8.5315
	1d	6.6244	2d	7.2359	3d	9.1014
	1e	6.6249	2e	7.2907	3e	9.5067
6	1a	6.5574	2a	6.6629	3a	7.9684
	1b	6.6082	2b	6.7540	3b	8.0562
	1c	6.6215	2c	7.0059	3c	8.3550
	1d	6.6239	2d	7.1796	3d	8.8221
	1e	6.6246	2e	7.2607	3e	9.2636
	1f	6.6249	2f	7.2952	3f	9.5488

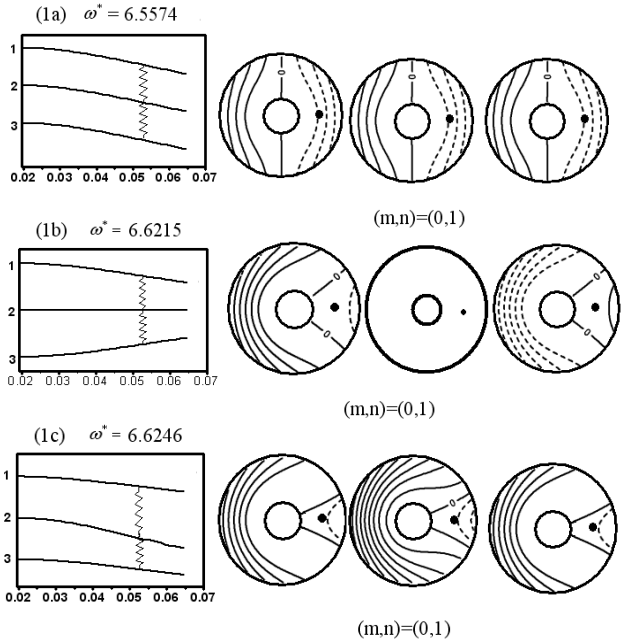

Fig. 3. First set (n=1) of natural modes of a stacked 3-disk system.

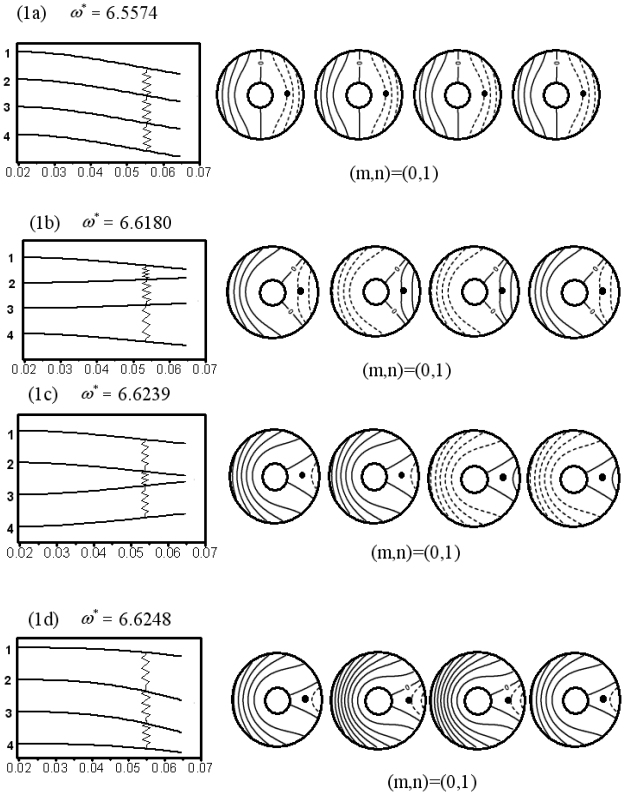

Fig. 4. First set (n=1) of natural modes of a stacked 4-disk system.

phase but opposite to the bottom two disks. At the fourth mode, all disks vibrate in phase, but the middle two disks have double magnitude than the outer two.

It has been noticed from Figs. 3 and 4 that the natural frequencies of coupled disks are just slightly deviated from the corresponding single disk's natural frequency, for the shown examples 1.0%. These results show no surprise because a single weak point restraint is never enough to significantly shift a disk's natural frequencies. The mode shapes are, however, tremendously different from a disk's n=1 mode. It is hence realized that the significant effects of spring coupling, even for weak coupling, are the mode shapes rather than the natural frequencies.

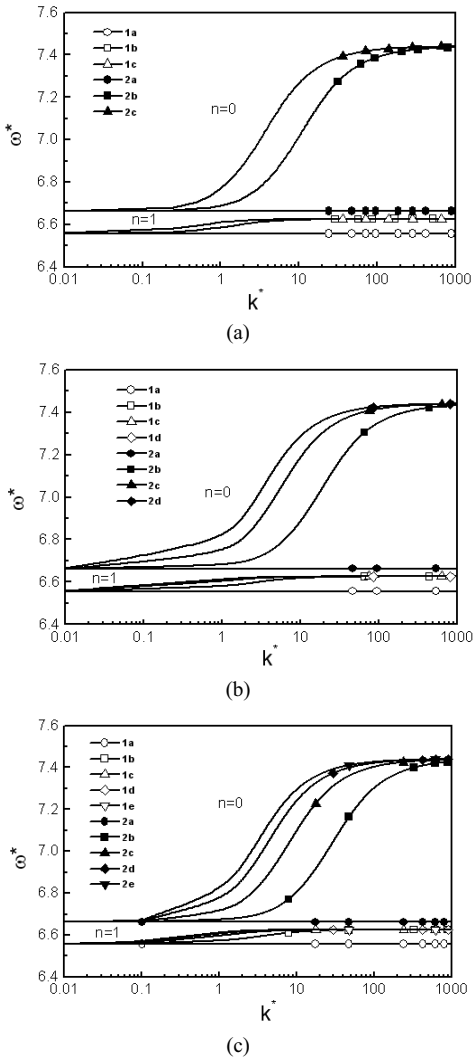

Fig. 5. Variations of natural frequencies with spring constant for (a) 3-disk, (b) 4-disk, and (c) 5-disk.

Fig. 5 shows effects of spring constant on the changes of natural frequencies for the 3, 4, and 5-disk cases. As seen, when k^* increases ω* increases as well but it appears that the higher frequency modes (n=0) are influenced more than the lowest ones (n=1). The authors have calculated for n up to 4 and concluded from the numerical results that higher n (>1) modes are always affected more than lower n modes. When k^* exceeds 1000, the springs act as rigid connections. Fig. 6 shows the effects of spring location. As expected, the outer the springs are located, the

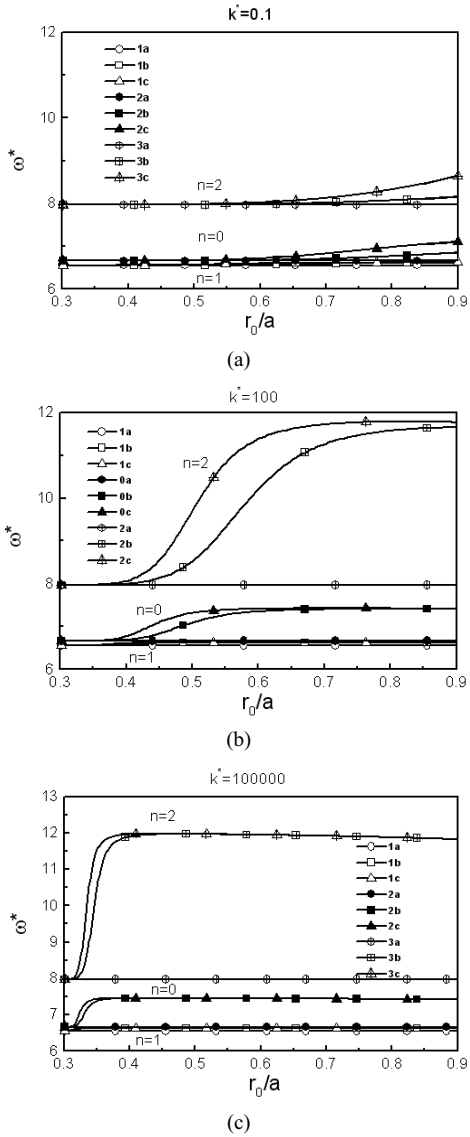

Fig. 6. Variations of natural frequencies with spring location for (a) 3-disk, (b) 4-disk, and (c) 5-disk.

greater the effects on natural frequencies changes that result. Similar to the k^* effect, the higher n modes are influenced more than the lower n modes. Note that the above figures only showed the modes associated with zero nodal circle (m=0). For m=1,2 a similar phenomenon was observed but not shown in the paper for brevity.

Fig. 7 is intended to show the spinning effects on disks' natural frequencies. Three different spring constants are illustrated to, respectively, denote weak, mild, and strong coupling. For very weak coupling (k^* =0.1), the stacked disks' natural frequencies almost coincide with those of a single disk (dotted curves). At mild coupling, there are more starting points at Ω^*=0 than a single disk. It is sometimes called the bifurcation of natural frequencies. These points draw frequency loci as the spinning speed increases. The loci are seen veering and passing through the crossings of a single disk's loci. It is a peculiar feature found in rotating structures, as investigated by many authors [13, 15, 16]. For strong coupling, the phenomenon remains and the only difference is the curves are separated farther from the beginning.

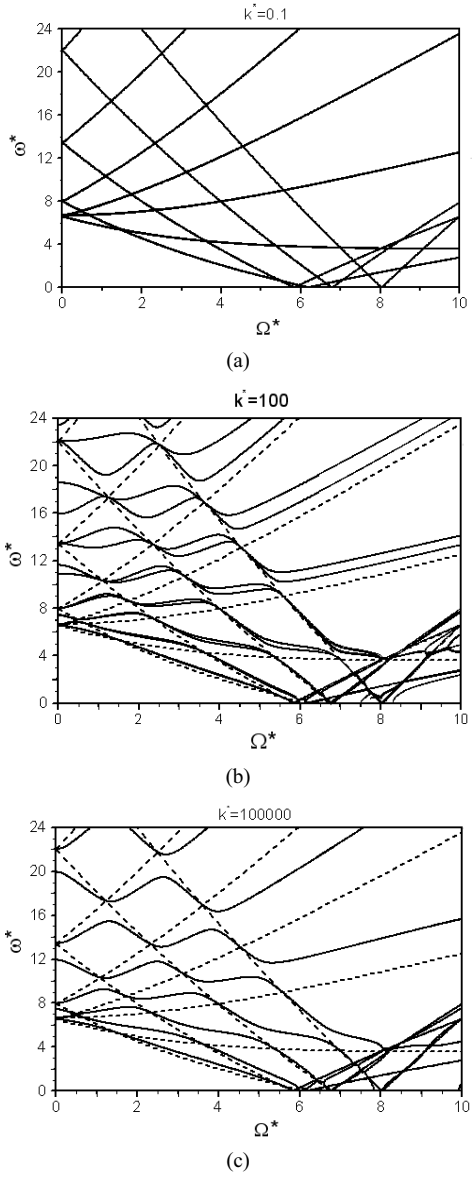

Fig. 7. Frequency loci with respect to spinning speed for (a) weak coupling,(b) mild coupling, and (c) strong coupling.

4. Concluding remarks

A stacked multi-disk with springs intervening among disks was investigated. It could simulate a computer disk-head assembly. The equations of motion for a spinning disk were first derived and the receptance method was applied to join disks and springs. A recursive equation for natural frequencies was then derived. Numerical cases were illustrated and the results revealed the following conclusions. (i) Each clustering frequency evolves into p distinct natural frequencies as p disks are stacked together through spring coupling. It is also referred to as the bifurcation of natural frequencies. (ii) The springs tend to affect slightly the natural frequencies, but the variations of mode shapes are very significant. That is, the system's natural frequencies may not be altered by the heads' weak coupling, but the mode shapes can be very different. It implies that each disk may deform very differently and cause concerns on read/write capability. (iii) The spring coupling has a greater effect on the higher modes than on the lower modes. A similar phenomenon occurs at spring location effects. (iv) The spinning effects are found not only to change the natural frequencies but also to pull the frequencies loci passing through the crossings of the single disk's natural frequencies.

References

[1] H. Lamb and R. V. Southwell, The vibrations of a spinning disk, *Proceedings of the Royal Society* 99 (1921) 272-280.

[2] C. D. Mote, Free vibrations of initially stressed circular disks, *J. Engi. for Industry* 87 (2) (1965) 258-264.

[3] G. C. Adams, Critical speeds for a flexible spinning disk, *Int. J. Mech. Sci.* 29 (8) (1987) 525-531.

[4] R. C. Benson and D. B. Bogy, Deflection of a very flexible spinning disk due to a stationary transverse load, *ASME J. Appl. Mech.* 45 (1978) 636-642.

[5] K. J. Stahl and W. D. Iwan, On the response of a two-degree-freedom rigid disk with a moving massive load, *ASME J. Appl. Mech.* 40 (1973) 114-120.

[6] K. J. Stahl and W. D. Iwan, On the response of an elastically supported rigid disk with a moving massive load, *Int. J. Mech. Sci.* 15 (1973) 535-546.

[7] I. Y. Shen and C. D. Mote, On the mechanisms of instability of a circular plate under a rotating spring-mass-dashpot system, *J. Sound Vibr.* 48 (20) (1991) 307-318.

[8] J. S. Chen and D. B. Bogy, Effects of load parameters on the natural frequencies and stability of a flexible spinning disk with a stationary load system, *ASME J. Appl. Mech.* 59 (1992) 230-235.J. S. Chen and D. B. Bogy, Natural frequencies and stability of a flexible spinning disk-stationary load system with rigid-body tilting, *ASME J. Appl. Mech.* 60 (1993) 470-477.

[9] S. C. Huang and W. J. Chiou, Modeling and vibration analysis of spinning-disk and moving-head assembly in computer storage system, *ASME J. Vibr. Acous.* 119 (2) (1997) 185-191.

[10] I. Y. Shen and C. P. R. Ku, A nonclassic vibration analysis of a multiple rotating disk and spindle assembly, *ASME J. Appl. Mech.* 64 (1997) 165-174.

[11] I. Y. Shen, Closed-form forced response of a damped, rotating, multiple disks/spindle system, *ASME J. Appl. Mech.* 64 (1997) 343-352.

[12] C. O. Orgun and B. H. Tongue, Mode localization in coupled circular plates, *ASME J. Vibr. Acous.* 116 (1994) 555-561.

[13] C. O. Orgun and B. H. Tongue, On localization in coupled spinning, circular plates, *ASME J. Vibr. Acous.* 116 (1994) 555-561.

[14] S. C. Huang and B. S. Hsu, Theory of receptance applied to modal analysis of a spinning disk with interior multi-point supports, *ASME J. Vibr. Acous.* 114 (1992) 468-476.

[15] S. C. Huang and B. S. Hsu, Modal analysis of a spinning cylindrical shell with interior point of circular line supports, *ASME J. Vibr. Acous.* 115 (1993) 535-543.

[16] S. C. Huang and C. H. Wu, Frequency analysis of a rotating plate with external beam-supports, *J. Sound Vibr.* 210 (4) (1998) 415-429.

[17] S. M. Vogel and D. W. Skinner, Natural frequencies of transversely vibrating uniform annular plates, *ASME J. Appl. Mech.* 32 (1965) 926-931.

[18] A. W. Leissa, Vibration of Plates, Scientific and technical information division National Aeronautics and Space Administration, (1969).